A mechanistic model of the regulation of division timing by the circadian clock in cyanobacteria

Po-Yi Ho[1,3], Bruno M.C. Martins[2,4], and Ariel Amir[1,*]

[1]John A. Paulson School of Engineering and Applied Sciences, Harvard University, Cambridge, MA, USA
[2]Sainsbury Laboratory, University of Cambridge, Cambridge, UK
[3]Present address: Department of Bioengineering, Stanford University, Stanford, CA, USA
[4]Present address: School of Life Sciences, University of Warwick, Coventry, UK
[*]Correspondence: arielamir@seas.harvard.edu

ABSTRACT   The cyanobacterium *Synechococcus elongatus* possesses a circadian clock in the form of a group of proteins whose concentrations and phosphorylation states oscillate with daily periodicity under constant conditions (1). The circadian clock regulates the cell cycle such that the timing of cell divisions is biased towards certain times during the circadian period (2–5), but the mechanism underlying this phenomenon remains unclear. Here, we propose a mechanism in which a protein limiting for division accumulates at a rate proportional to cell volume growth and modulated by the clock. This "modulated rates" model, in which the clock signal is integrated over time to affect division timing, differs fundamentally from the previously proposed "gating" concept, in which the clock is assumed to suppress divisions during a specific time window (2, 3). We found that while both models can capture the single-cell statistics of division timing in *S. elongatus*, only the modulated rates model robustly places divisions away from darkness during changes in the environment. Moreover, within the framework of the modulated rates model, existing experiments on *S. elongatus* are consistent with the simple mechanism that division timing is regulated by the accumulation of a division limiting protein in phase with genes whose activity peaks at dusk.

SIGNIFICANCE   Circadian clocks affect many aspects of cell physiology, including metabolism, gene expression, and cell cycle progression. However, the underlying mechanisms remain unclear. Here, we analyzed single-cell data of cell growth and division in the cyanobacterium *Synechoccocus elongatus* and constructed mathematical models to describe the statistics of division timing in strains with and without a circadian clock. Our analysis and modeling tentatively rule out mechanisms in which cells act quickly in response to signals from the clock, and suggest instead that a simple molecular mechanism in which cells integrate the clock signal over time is sufficient to describe existing experiments. Our work establishes a framework to analyze future single-cell experiments to probe the molecular mechanisms underlying the regulation of cell physiology by circadian clocks.

INTRODUCTION

How microorganisms regulate the timing of cell division is a fundamental problem in biology (6). Exploiting advances in microfluidics, recent works have shown that several species of bacteria, including *Escherichia coli* and *Bacillus subtilis*, divide after adding on average a constant size from birth to division at the single-cell level (7, 8). Other microorganisms, including the eukaryotic budding yeast *Saccharomyces cerevisiae* and the archaeon *Halobacterium salinarum*, were also shown to follow the same "adder" strategy to regulate division timing and control cell size, despite drastically different physiology (9, 10). The adder model is therefore a successful phenomenological model to describe when microorganisms divide as a function of their size (11, 12). However in cyanobacteria such as *Synechococcus elongatus*, division timing is also a function of the circadian clock (2).

S. elongatus cells possess a circadian clock in the form of three core clock proteins (the Kai proteins) whose concentrations and phosphorylation states oscillate with daily periodicity under constant conditions (1). The timing of the clock is not affected by cell divisions, but the clock affects division timing such that divisions occur more frequently during certain times of the circadian period (2–5). Specifically, the clock appears to bias divisions away from dawn and dusk (5), avoiding potentially deleterious effects of dividing during darkness (13). How the clock affects division timing in *S. elongatus* has recently been

measured at the single-cell level (5), but the underlying mechanism remains unclear. Here, we developed a mechanistic model for how the clock affects division timing in *S. elongatus* by extending the adder model to include the effects of a circadian clock.

Our model supposes that a protein limiting for division accumulates at a rate proportional to cell volume growth but modulated by the circadian clock. Our "modulated rates" model, in which the clock affects division timing by integrating the clock signal over time, differs fundamentally from the often considered "gating" model, in which the clock affects the instantaneous probability to divide. By formulating the two models using simple dynamics with coarse-grained stochasticity, we found that the modulated rates model better describes the statistics of division timings in existing experiments. By investigating how the models respond to environmental perturbations, we found that the modulated rates model more robustly places divisions away from dawn and dusk. Finally, by comparing the modulated rates model to existing experiments, we found that existing experiments are consistent with a simple molecular mechanism for how the clock regulates division timing.

METHODS

Here, we provide details for the methods used to analyze the models. The definition of variables and referenced equations appear later in the Results section, where we elaborate on the model itself.

Numerical simulations of the models

The deterministic generation time was determined by numerically integrating the equations for the accumulation of divisors, Eqs. 3 or 7. The stochastic generation time is obtained via Eq. 6. Cell volume is calculated according to Eqs. 1-2 and is divided in half at division. The process is repeated for at least 10^5 generations, following only one of the newborn cells at division. To describe the distribution of circadian phases at birth under LL, a similar method was used to track division events of a growing colony (SM Section 3).

Determination of the best fit values for model parameters

The best fit value of r in Eq. 3 was determined as follows. For a given r, σ in Eq. 6 was chosen to match the CV of l_b. The resulting values of σ agree well with that inferred from the difference in sibling generation times when ignoring the contribution from differences in cell sizes at birth due to noisy asymmetric divisions (SM Section 2). Then, the best fit value of r for the clock-deletion strain under 16:8 LD was chosen to minimize the sum of squared residues between model predictions and experimental observations for $p(\theta_b)$ and $p(t_d)$, with bin size corresponding to the experimental time resolution (0.75 h under LL and 1 h under LD). The best fit values of A and φ for the wild type strain under LD were determined by minimizing the same quantity. For the wild type strain under LL, the best fit values were chosen to minimize the sum of squared residues in the correlations between t_d and θ_b, binned according to θ_b with bin size corresponding to the experimental time resolution. Table S1 summarizes the best fit values of all parameters obtained.

Determination of the goodness of fit

The goodness of fit of the models and the errors on the best fit values of the model parameters can be estimated by comparing the residue between the best fit predictions (best residue) and that between the predictions of the divisor accumulation model without a clock (worst residue). To determine the error bars on the best fit values, we held other parameters constant and scanned the parameter in question until the residue becomes larger than 5% the difference between the best and worst residue. We determined error estimates to the decimal place for A, and to the hour for φ and the half-life corresponding to r.

RESULTS AND DISCUSSION

Modeling the growth and division of *S. elongatus* cells

To construct a model to describe how the clock affects division timing, we analyzed data from Ref. (5), which observed the growth and division of single cells for a wild type strain of *S. elongatus* and a strain whose *kaiBC* locus was deleted, referred to here as the clock-deletion strain. Since *S. elongatus* cells require light to grow, they were grown and imaged under constant light (LL) or periodic cycles of light and darkness (12:12 LD, i.e. 12 hours of light with a graded intensity profile, followed by 12 hours of darkness, and 16:8 LD) to probe the effects of the clock on division timing under different environments. For each cell, its length at birth l_b and division l_d and its generation time (the time between birth and division) t_d were measured. Before imaging, the cells were grown under 12:12 LD to entrain and synchronize the activity of the clock to the environmental light conditions. The circadian phase θ corresponding to the internal, subjective time of day encoded by the clock can then be assumed to be set to the environmental light-dark cycle. We defined $\theta = 0$ h to be dawn, or the beginning of the period

under light. Each cell can then be assigned a circadian phase at birth θ_b. We analyzed the distributions of (denoted $p\left(\cdot\right)$) and correlations among the four stochastic variables $(l_b, l_d, t_d, \theta_b)$, and compared these statistics of division timing to those generated by our models (Fig. 1). Similar approaches have led to insights on other aspects of microbial and also eukaryotic cell cycles, including how DNA replication might be coupled to division timing (7, 8, 10, 12, 14–19).

We first modeled the growth mode of single cells, which has significant implications for cell cycle regulation (see Discussion) (12, 14). The growth mode of *S. elongatus* cells can be approximated to be exponential, with a rate dependent on the environmental light intensity (4, 5). We therefore modeled the growth of volume V as

$$\frac{dV}{dt} = \lambda\left(\theta\right)V. \tag{1}$$

The growth rate $\lambda\left(\theta\right)$ may depend on the light intensity, which is a function of θ for the periodic environments under consideration. Under LL, $\lambda\left(\theta\right)$ can be approximated as constant for our purposes, although in reality it varies up to $\approx 5\%$ with the circadian phase (5). Under LD, $\lambda\left(\theta\right)$ is approximately proportional to the environmental light intensity. The experimental light intensity profile is sinusoidal during the period under light. We therefore modeled $\lambda\left(\theta\right)$ as

$$\lambda\left(\theta\right) = \begin{cases} \lambda_0 \sin\left(\pi\frac{\theta}{T_L}\right) & \theta < T_L \\ 0 & \theta \geq T_L \end{cases}, \tag{2}$$

where λ_0 is the maximum growth rate and T_L is the duration of the period under light. λ_0 and T_L are known parameters. For our analyses, we use cell volume and cell length interchangeably since volume can be well approximated as proportional to cell length in rod-shaped bacteria that grow by elongation such as *S. elongatus* (20). Experimentally, cells divide approximately symmetrically with small fluctuations in the division ratio (i.e. 0.51 ± 0.02 in the data set for wild type cells under LL). We assumed perfectly symmetrical divisions in our models.

[Figure 1 about here; moved to end of manuscript by `endfloat`.]

Divisor accumulation can describe division timing in a clock-deletion strain

To construct a basic model of division timing without a clock, we considered the experiments on the clock-deletion strain. Under LL, the clock-deletion strain behaves, with minor deviations, like several other microbes whose cells appear to add a constant size from birth to division on average (Fig. 2a) (7–10, 17, 21). Inspired by models that sought to describe such single-cell correlations and their mechanistic implications (SM Section 1) (15, 22–24), we considered the following "divisor accumulation" model. Its basic component is the accumulation of a divisor protein limiting for division, whose amount is denoted by X, at a rate proportional to volume growth,

$$\frac{dX}{dt} = k\frac{dV}{dt} - rX. \tag{3}$$

Here, r is the degradation rate of the divisor. Division occurs upon the accumulation of a threshold amount X_0 of divisors. Divisors are consumed during division so that the amount of divisors is zero at birth, denoted by $t = 0$. That is,

$$X\left(t = 0\right) \quad = \quad 0, \tag{4}$$

$$X\left(t = t_0\right) \quad = \quad X_0. \tag{5}$$

The resetting of divisors could be describing a scenario similar to the disassembly of the divisome in *E. coli* (25). In Eq. 5, t_0 is the deterministic generation time. On top of the deterministic dynamics of Eqs. 3-5, we implement a time-additive noise to model the stochasticity in division timing due to, for example, noise in gene expression (e.g. Refs. (14, 26)). The stochastic generation time t_d is

$$t_d = t_0 + \sigma\xi, \tag{6}$$

where ξ is a normal random variable with zero mean and unit standard deviation, and σ is the magnitude of the time-additive noise. In Eqs. 3 and 5, we set $k = 1$ and $X_0 = 1$ because we were not interested in the absolute magnitudes of the concentration of the divisor or the cell volume. Instead, we analyzed statistics such as coefficient of variations (CV, the standard deviation divided by the mean) and correlations coefficients that are independent of the absolute magnitudes. The free parameters of the model are r and σ. The best fit value of r was determined for the clock-deletion strain under 16:8 LD, which admitted a more precise determination of r than other conditions (Methods). The resulting value of r was 0.025 ± 0.006 h^{-1}, which corresponds to a half life of approximately 28 h, and was assumed to be the same for all other conditions. σ was determined separately for

each condition, analogous to the fact that bacterial cells grown under different conditions might exhibit different magnitudes of stochasticity in division timing (8). Although the model does not specify the molecular identity of the divisor, it might be describing, for example, the accumulation of FtsZ, a protein implicated for cell division in some bacteria (18, 27, 28).

We then compared the divisor accumulation model, Eqs. 1-6, with the experiments on the clock-deletion strain. Under LL, the model predicts close to no correlations between $l_d - l_b$ and l_b, in approximate agreement with experiments (Fig. 2a). Although the experimentally observed correlation was more negative, the difference did not affect the modeling predictions and comparisons below (SM Section 1). Moreover, since the model does not contain a clock, t_d is independent of θ_b, again in agreement with experiments (Fig. 2b). Under LD, experiments showed that the value of $p(\theta_b)$ is small near dawn. The model captures this observation because the divisors degrade, so that cells typically do not have enough divisors to divide immediately after dawn (Fig. 2ce, SM Section 1). Under LD, $p(t_d)$ is bimodal because some cells divide before reaching a period of darkness (short-generation cells), whereas other cells must wait through a period of darkness before division (long-generation cells). The model is able to capture the mean generation times of both short- and long-generation cells (Fig. 2df, SM Section 1). Moreover, the model predictions for the distributions of and the correlations between the other stochastic variables also agree with experiments (Fig. S4abc). Taken together, divisor accumulation is a simple mechanistic model that can capture the statistics of division timing in the clock-deletion strain.

[Figure 2 about here; moved to end of manuscript by `endfloat`.]

Divisor accumulation with modulated rates can describe division timing with a circadian clock

To construct a mechanistic model for how the clock affects division timing, we incorporated the effects of the clock into the divisor accumulation model, and compared the resulting model with the experiments on the wild type strain. Under LL, the clock generates correlations between θ_b, l_b, and t_d that cannot be captured by the divisor accumulation model without a clock (Fig. 3ab). We therefore considered a modulated rates model where the rate of accumulation of the divisor is modulated by a periodic function $y(\theta)$,

$$\frac{dX}{dt} = \frac{dV}{dt} y(\theta) - rX. \tag{7}$$

$y(\theta)$ could be describing, for example, the approximately sinusoidal promoter activity of FtsZ under LL (29). We therefore assumed the following sinusoidal form,

$$y(\theta) = 1 + A(\cos(\omega t - \pi\varphi/12) - 1), \tag{8}$$

where $\omega = 2\pi/(24\text{ h})$, and A and φ are the magnitude and phase offset of the modulation. The sinusoidal form is reasonable also under periodic LD conditions because the activity of the *kaiBC* promoter, and presumably other downstream genes with circadian oscillations, remains sinusoidal during the day (30). We chose $y(\theta)$ to have a maximum of one, since the absolute magnitude of $y(\theta)$ does not affect the statistics of division timing. We also enforced $X \geq 0$. We determined the values of the free parameters A and φ for each condition (Methods, SM Section 2), reflecting the fact that the molecular players that implement $y(\theta)$ may depend on environmental light conditions (31). In particular, clocks are entrained to the environment relatively quickly (30). In the 16:8 LD experiments, almost all (90%) of recorded division events occurred after the first day of imaging, and hence correspond to cells that should by then be entrained to 16:8 LD. We therefore assumed A and φ to be constant also for 16:8 LD.

Despite its simplicity, the modulated rates model can capture the correlations between t_d and θ_b under LL (Fig. 3a). The slight mismatch between model and experiment does not affect the subsequent modeling comparisons. Furthermore, the model without further adjustments also captures the correlations between $l_d - l_b$ and l_b ($\rho = -0.32 \pm 0.05$, Pearson correlation coefficient with 95% confidence interval; Fig. 3b), which is more negative than in the clock-deletion strain ($\rho = -0.21 \pm 0.05$). Such correlations arise because, within the model, cells that are larger at birth likely have just grown through periods where the divisor accumulation rate was repressed by $y(\theta)$, and will therefore tend to grow through periods of derepressed divisor accumulation. The size increments between birth and division of larger cells will therefore be smaller than average (SM Section 1). The model also captures the other statistics of division timing (Fig. S4d). In particular, because the statistics were not collected over lineages but over growing populations, $p(\theta_b)$ is not the same as the distribution of circadian phases at division $p(\theta_d)$, where θ_d is defined as $(\theta_b + t_d)$ mod 24. The model captures both distributions after taking into account the details of the ensemble (SM Section 4). Moreover, the model also captures correlations between distantly related cells such as the cousin-cousin correlations between generation times (SM Section 4).

The model can also describe the division timing of the wild type strain under LD (Fig. 3cd, Fig. S4ef). Specifically, it captures that wild type cells, compared to cells of the clock-deletion strain, began to divide later after dawn, and stopped

dividing sooner before dusk (Fig. 3c). Within the model, divisions are biased to occur away from darkness because $y(\theta)$ peaks near the mid-point of the light period (Fig. 1a). The model also predicts that the clock will decrease (increase) the mean generation time of the short- (long-) generation cells, in agreement with experiments (Fig. 3d). In summary, divisor accumulation with modulated rates, Eq. 7, is a model with two free parameters (A and φ) that can describe the statistics of division timing in wild type *S. elongatus* under both constant and periodic environments (Fig. 3 and Fig. S4).

[Figure 3 about here; moved to end of manuscript by `endfloat`.]

The modulated rates model robustly places divisions away from darkness, whereas the gating model does not

The modulated rates model, in which the clock signal is integrated over time to affect division timing, differs fundamentally from the widely considered gating hypothesis, which assumes that the clock suppresses divisions during a specific time window (2, 3). We next sought to distinguish between the two hypotheses by incorporating the gating hypothesis into the framework of the divisor accumulation model, and comparing the predictions of the two models. In our gating model, divisors accumulate without modulation by the clock, as in Eq. 3. However, only a fraction $y(\theta)$ of the accumulated divisors is active in contributing to reaching the threshold. That is,

$$\tilde{X} = X y(\theta), \tag{9}$$

where $\tilde{X}$ is the amount of active divisors. A threshold amount of active divisors triggers division,

$$\tilde{X}(t = t_0) = X_0. \tag{10}$$

All other aspects of the gating model are the same as the modulated rates model. The gating function $y(\theta)$ could be, for example, a step function equal to zero during the window of suppressed division and one otherwise, which is exactly the case considered in Ref. (3). To compare the gating and the modulated rates models without additional differences, we considered the case where $y(\theta)$ is sinusoidal as in Eq. 8. By using the same fitting procedure as for the modulated rates model, we found that the gating model can also capture the effects of the clock on the statistics of division timing (Fig. S6). To more clearly distinguish between the two hypotheses, we next sought to understand how the two models differ qualitatively.

First, the best fit values of φ suggest that the effect on division timing by the clock is implemented by different molecular players in the two models. For the modulated rates model, one mechanistic interpretation is that $y(\theta)$ describes the promoter activity of the divisor. In this case, the value of φ is related to the phase at the peak of the concentration of the divisor (SM Section 1). Specifically, we found that the divisor concentration peaks approximately 12 ± 1 hours after dawn under 12:12 LD (Table 1), suggesting that within the modulated rates model, $y(\theta)$ is implemented by molecular players whose activity peaks at dusk. For the gating model, one mechanistic interpretation is that $y(\theta)$ describes the concentration of an effector that transmits the signal of the clock to affect division timing, since the effector acts immediately to affect the fraction of active divisors. In this case, the best fit values of φ in the gating model imply that the effector concentration peaks 8 hours after dawn under 12:12 LD (Table 1). Therefore, within the gating model, $y(\theta)$ would be implemented by molecular players whose activity does not peak at dusk, in contrast with the modulated rates model. This difference between the two models is reminiscent of the different classes of promoters whose peaking time cluster around either dusk or dawn (32), although the difference in peaking times here is not more than 4 hours. Analysis of data in more conditions using the above approach could inform the search for the molecular players that determine division timing in *S. elongatus*.

In addition, the best fit values of φ are more parsimoniously interpreted in the modulated rates model. Experiments have shown that for different values of T_L (Eq. 2), the activity of the *kaiBC* promoter shifts in circadian phase such that the phase at the peak increases by $T_L/2$, or "mid-day tracking" (30). Consistent with this observation, the best fit value of φ under 16:8 LD is two hours more than that under 12:12 LD in the modulated rates model (Table 1). Also in the modulated rates model, the best fit value of φ under LL is the same as that under 12:12 LD, consistent with the fact that the clock was entrained under 12:12 LD (Table 1). In contrast, the best fit value of φ in the gating model under LL is five hours different from that under 12:12 LD, suggesting that the molecular players in the gating model do not follow a mid-day tracking activity. Note, however, that the experiments in Ref. (30) were done with on-off light intensity profiles without the sinusoidal dependence used in Ref. (5). Therefore, further experiments to determine the activity of the Kai proteins, and other potential modulators of division timing, would help verify the above distinction between the two models.

The differences between the two models in predictions involving φ arise from the difference between integrating a signal over time, and acting on the signal instantaneously. By taking the derivative of Eq. 9, the gating model can be rewritten as,

$$\frac{d\tilde{X}}{dt} = \frac{dV}{dt} y - r\tilde{X} + X \frac{dy}{dt}, \tag{11}$$

which is equivalent to the modulated rates model for the variable $\tilde{X}$ with an extra term $X\,(dy/dt)$. When the degradation rate is small compared to the growth rate, as is the case here, X approximately scales like dV/dt. The extra term therefore approximately modulates the rate of divisor accumulation by both y and the derivative of y. The form of the extra modulation explains why both models can capture the effects of the clock on division timing, albeit with quantitatively different predictions involving the best fit values of φ.

Importantly, the modulated rates model predicts no divisions during darkness, whereas the gating model can lead to divisions during darkness without growth. The latter case occurs when enough divisors have accumulated, but not enough are active according to the gating function $y\,(\theta)$. Divisions can then occur just by the passage of time, without cell growth, and the consequent activation of divisors with increasing $y\,(\theta)$. The above scenario can be demonstrated in a numerical simulation using the best fit parameters under 16:8 LD, and tracking the division events for cells entrained under 16:8 LD but imaged during a cycle where the light is turned off abruptly during the day. The gating model predicts that a noticeable fraction of cells will divide during darkness in this scenario, whereas the modulated rates model predicts no divisions during darkness (Fig. 4a). Divisions in darkness have indeed not been observed experimentally. However, it may be that cells possess additional mechanisms to abort divisions during darkness, regardless of how the clock affects division timing. One way to distinguish between the two models while circumventing this possibility is to decrease the light intensity abruptly to a small but non-zero value. In this case, the gating model predicts that a larger fraction of cells will divide afterwards (Fig. 4b). We note the caveat that the clock will likely be re-entrained by the abrupt change in light intensity, and hence, $y\,(\theta)$ will be affected on longer time scales. Nevertheless, on the shorter time scale shortly after the change in light intensity, our predictions will hold. The above difference between the two models could be relevant for cells in nature facing fluctuations in environmental light intensity (13). The experimental realization of the scenario would be one way to directly differentiate the two models.

[Table 1 about here; moved to end of manuscript by `endfloat`.]

[Figure 4 about here; moved to end of manuscript by `endfloat`.]

CONCLUSION

How cyanobacteria regulate division timing has been studied for decades, but how and why the clock regulates division timing remain unclear (2, 4, 5, 33). One widely considered mechanism is that of gating, where the signal from the clock is assumed to suppress divisions in a specific time window (2, 3). Here, we proposed a different mechanism of modulated rates, where the signal from the clock is integrated over time to affect division timing. Biologically, the gating model could correspond to a post-translational mechanism while the modulated rates model could correspond to a transcriptional mechanism.

To distinguish between the two mechanisms, we formulated a simple framework that describes how cell volume growth, the environmental light profile, and the internal circadian clock together determine division timing. Our framework differs from existing ones in both formalism and structure. Ref. (4) modeled the relation between the progression of the circadian phase and that of division timing with a general nonlinear map. Ref. (33) studied a model in which the generation time is determined by a linear combination of the previous generation time and an oscillatory function of the circadian phase. The above approaches did not consider the feedback of cell size on division timing. However, for exponentially growing cells such as those of *S. elongatus*, timing divisions without feedback from cell size fails to maintain a homeostatic average cell size (14). Ref. (5) accounted for the effects of cell size regulation by modeling the instantaneous probability to divide as a function of cell size multiplied by the growth rate and a periodic coupling function of the circadian phase (34). The approach of Ref. (5) can describe the experimentally observed statistics of division timing under LL. However, the coupling function fitted to LL data cannot capture the low density of divisions in the early hours of the light period under LD (SM Section 5). It is also not straightforward to parametrize the coupling function to gain an understanding of the underlying molecular mechanism, which will require further work. Our models specify division timing via simple deterministic dynamics and implement stochasticity via a coarse-grained noise term (12). The simplicity provides mechanistic insights by describing how the clock affects division timing via two parameters with mechanistic interpretations.

With our framework, the modulated rates model appears to be more consistent with existing experiments than the gating model. Moreover, existing data is consistent with the simple mechanism that division timing is regulated by the accumulation of a division limiting protein in phase with genes whose activity peaks at dusk. Together with further single-cell level experiments, especially those with genetic perturbations such as those in Ref. (3) (see SM Section 5 for example), our simple and illustrative modeling framework will be useful in unraveling how the clock regulates division timing.

AUTHOR CONTRIBUTIONS

ACKNOWLEDGMENTS

REFERENCES

1. Johnson, C. H., C. Zhao, Y. Xu, and T. Mori, 2017. Timing the day: what makes bacterial clocks tick? *Nature Reviews Microbiology* 15:232–242.

2. Mori, T., B. Binder, and C. H. Johnson, 1996. Circadian gating of cell division in cyanobacteria growing with average doubling times of less than 24 hours. *Proceedings of the National Academy of Sciences* 93:10183–10188.

3. Dong, G., Q. Yang, Q. Wang, Y.-I. Kim, T. L. Wood, K. W. Osteryoung, A. van Oudenaarden, and S. S. Golden, 2010. Elevated ATPase Activity of KaiC Applies a Circadian Checkpoint on Cell Division in *Synechococcus elongatus*. *Cell* 140:529–539.

4. Yang, Q., B. F. Pando, G. Dong, S. S. Golden, and A. van Oudenaarden, 2010. Circadian Gating of the Cell Cycle Revealed in Single Cyanobacterial Cells. *Science* 327:1522–1526.

5. Martins, B. M. C., A. K. Tooke, P. Thomas, and J. C. W. Locke, 2018. Cell size control driven by the circadian clock and environment in cyanobacteria. *Proceedings of the National Academy of Sciences* 115:E11415–E11424.

6. Koch, A. L., 1995. Bacterial Growth and Form. Springer US.

7. Campos, M., I. V. Surovtsev, S. Kato, A. Paintdakhi, B. Beltran, S. E. Ebmeier, and C. Jacobs-Wagner, 2014. A Constant Size Extension Drives Bacterial Cell Size Homeostasis. *Cell* 159:1433–1446.

8. Taheri-Araghi, S., S. Bradde, J. T. Sauls, N. S. Hill, P. A. Levin, J. Paulsson, M. Vergassola, and S. Jun, 2015. Cell-Size Control and Homeostasis in Bacteria. *Current Biology* 25:385–391.

9. Soifer, I., L. Robert, and A. Amir, 2016. Single-Cell Analysis of Growth in Budding Yeast and Bacteria Reveals a Common Size Regulation Strategy. *Current Biology* 26:356–361.

10. Eun, Y.-J., P.-Y. Ho, M. Kim, S. LaRussa, L. Robert, L. D. Renner, A. Schmid, E. Garner, and A. Amir, 2017. Archaeal cells share common size control with bacteria despite noisier growth and division. *Nature Microbiology* 3:148–154.

11. Willis, L., and K. C. Huang, 2017. Sizing up the bacterial cell cycle. *Nature Reviews Microbiology* 15:606–620.

12. Ho, P.-Y., J. Lin, and A. Amir, 2018. Modeling Cell Size Regulation: From Single-Cell-Level Statistics to Molecular Mechanisms and Population-Level Effects. *Annual Review of Biophysics* 47:251–271.

13. Lambert, G., J. Chew, and M. J. Rust, 2016. Costs of Clock-Environment Misalignment in Individual Cyanobacterial Cells. *Biophysical Journal* 111:883–891.

14. Amir, A., 2014. Cell Size Regulation in Bacteria. *Physical Review Letters* 112.

15. Ho, P.-Y., and A. Amir, 2015. Simultaneous regulation of cell size and chromosome replication in bacteria. *Frontiers in Microbiology* 6.

16. Wallden, M., D. Fange, E. G. Lundius, O. Baltekin, and J. Elf, 2016. The Synchronization of Replication and Division Cycles in Individual E. coli Cells. *Cell* 166:729–739.

17. Logsdon, M. M., P.-Y. Ho, K. Papavinasasundaram, K. Richardson, M. Cokol, C. M. Sassetti, A. Amir, and B. B. Aldridge, 2017. A Parallel Adder Coordinates Mycobacterial Cell-Cycle Progression and Cell-Size Homeostasis in the Context of Asymmetric Growth and Organization. *Current Biology* 27:3367–3374.e7.

18. Si, F., G. L. Treut, J. T. Sauls, S. Vadia, P. A. Levin, and S. Jun, 2019. Mechanistic Origin of Cell-Size Control and Homeostasis in Bacteria. *Current Biology* 29:1760–1770.e7.

19. Lambert, A., A. Vanhecke, A. Archetti, S. Holden, F. Schaber, Z. Pincus, M. T. Laub, E. Goley, and S. Manley, 2018. Constriction Rate Modulation Can Drive Cell Size Control and Homeostasis in *C. crescentus*. *iScience* 4:180–189.

20. Zheng, H., P.-Y. Ho, M. Jiang, B. Tang, W. Liu, D. Li, X. Yu, N. E. Kleckner, A. Amir, and C. Liu, 2016. Interrogating theEscherichia colicell cycle by cell dimension perturbations. *Proceedings of the National Academy of Sciences* 113:15000–15005.

21. Sauls, J. T., D. Li, and S. Jun, 2016. Adder and a coarse-grained approach to cell size homeostasis in bacteria. *Current Opinion in Cell Biology* 38:38–44.

22. Harris, L. K., and J. A. Theriot, 2016. Relative Rates of Surface and Volume Synthesis Set Bacterial Cell Size. *Cell* 165:1479–1492.

23. Barber, F., P.-Y. Ho, A. W. Murray, and A. Amir, 2017. Details Matter: Noise and Model Structure Set the Relationship between Cell Size and Cell Cycle Timing. *Frontiers in Cell and Developmental Biology* 5.

24. Ghusinga, K. R., J. J. Dennehy, and A. Singh, 2017. First-passage time approach to controlling noise in the timing of intracellular events. *Proceedings of the National Academy of Sciences* 114:693–698.

25. Soderstrom, B., K. Skoog, H. Blom, D. S. Weiss, G. von Heijne, and D. O. Daley, 2014. Disassembly of the divisome in *Escherichia coli*: evidence that FtsZ dissociates before compartmentalization. *Molecular Microbiology* 92:1–9.

26. Sandler, O., S. P. Mizrahi, N. Weiss, O. Agam, I. Simon, and N. Q. Balaban, 2015. Lineage correlations of single cell division time as a probe of cell-cycle dynamics. *Nature* 519:468–471.

27. Sekar, K., R. Rusconi, J. T. Sauls, T. Fuhrer, E. Noor, J. Nguyen, V. I. Fernandez, M. F. Buffing, M. Berney, S. Jun, R. Stocker, and U. Sauer, 2018. Synthesis and degradation of FtsZ quantitatively predict the first cell division in starved bacteria. *Molecular Systems Biology* 14:e8623.

28. Mannik, J., B. E. Walker, and J. Mannik, 2018. Cell cycle-dependent regulation of FtsZ in *Escherichia coli* in slow growth conditions. *Molecular Microbiology* 110:1030–1044.

29. Mori, T., and C. H. Johnson, 2001. Independence of Circadian Timing from Cell Division in Cyanobacteria. *Journal of Bacteriology* 183:2439–2444.

30. Leypunskiy, E., J. Lin, H. Yoo, U. Lee, A. R. Dinner, and M. J. Rust, 2017. The cyanobacterial circadian clock follows midday in vivo and in vitro. *eLife* 6.

31. Piechura, J. R., K. Amarnath, and E. K. O'Shea, 2017. Natural changes in light interact with circadian regulation at promoters to control gene expression in cyanobacteria. *eLife* 6.

32. Vijayan, V., R. Zuzow, and E. K. O'Shea, 2009. Oscillations in supercoiling drive circadian gene expression in cyanobacteria. *Proceedings of the National Academy of Sciences* 106:22564–22568.

33. Mosheiff, N., B. M. C. Martins, S. Pearl-Mizrahi, A. Grunberger, S. Helfrich, I. Mihalcescu, D. Kohlheyer, J. C. W. Locke, L. Glass, and N. Q. Balaban, 2018. Inheritance of Cell-Cycle Duration in the Presence of Periodic Forcing. *Physical Review X* 8.

34. Osella, M., E. Nugent, and M. C. Lagomarsino, 2014. Concerted control of *Escherichia coli* cell division. *Proceedings of the National Academy of Sciences* 111:3431–3435.

SUPPLEMENTARY MATERIAL

An online supplement to this article can be found by visiting BJ Online at http://www.biophysj.org.
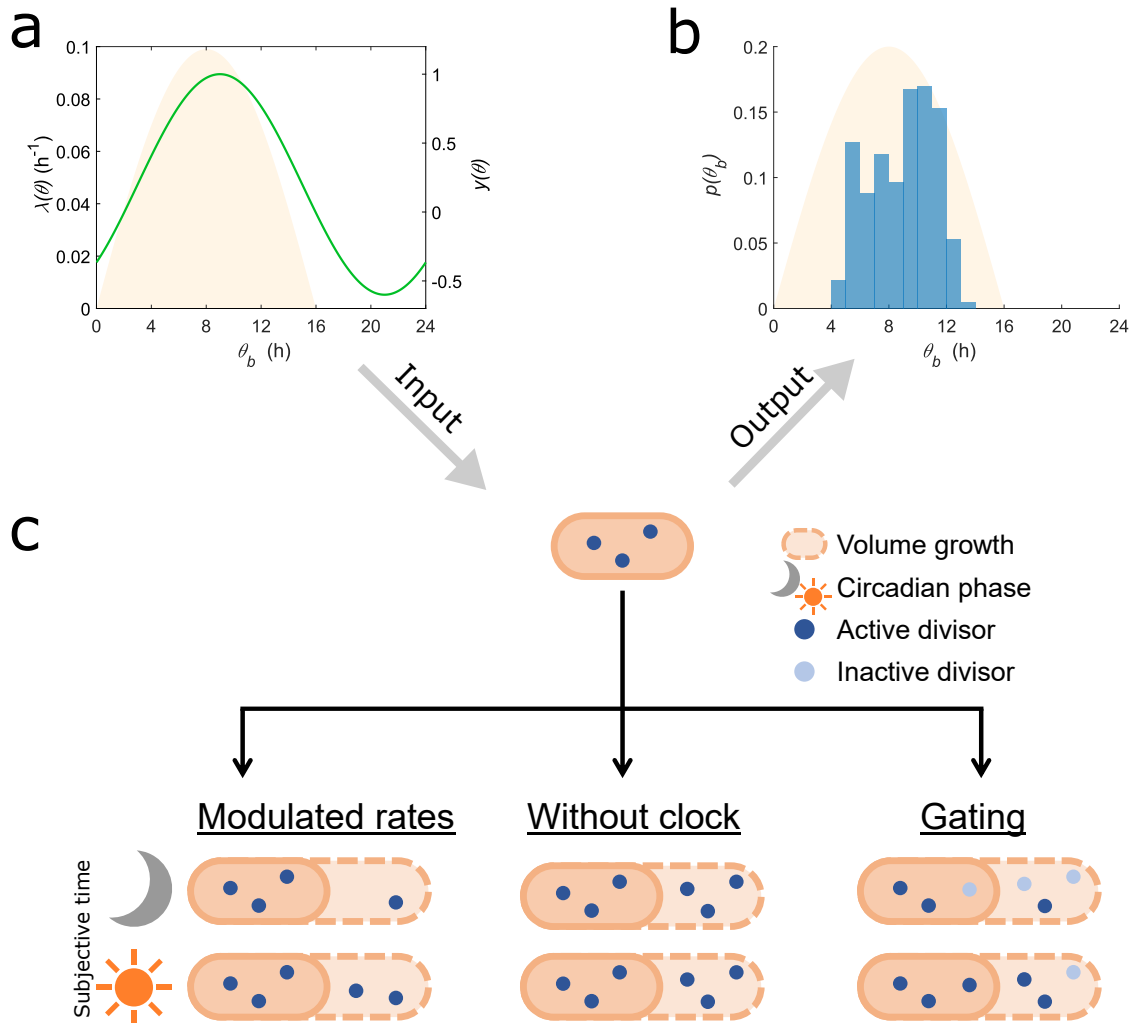
LIST OF FIGURES

Figure 1: Two models for the regulation of division timing by the circadian clock. Both models take as inputs (a) the environmental light-dark cycles ($\lambda(\theta)$, yellow shade) and a modulation function ($y(\theta)$, green line) that determines how the clock affects division timing to give as outputs (b) the single-cell distributions of and correlations among cell length at birth l_b and division l_d, the circadian phase at birth θ_b, and the generation time t_d. Shown is an experimentally observed distribution of θ_b for *S. elongtaus* under periodic conditions, showing that divisions occur away from dawn and dusk (5). (c) (Middle) The divisor accumulation model without the clock, Eq. 3. The divisor is accumulated at a rate proportional to volume growth, regardless of the underlying circadian phase as denoted by the moon and sun. (Left) The modulated rates model, Eq. 7. The divisor accumulation rate is modulated by the subjective time given by the clock. (Right) The gating model, Eq. 9. The divisor accumulation rate is not affected by the clock, but only a fraction of divisors, determined by the current circadian phase, is active towards reaching the threshold.
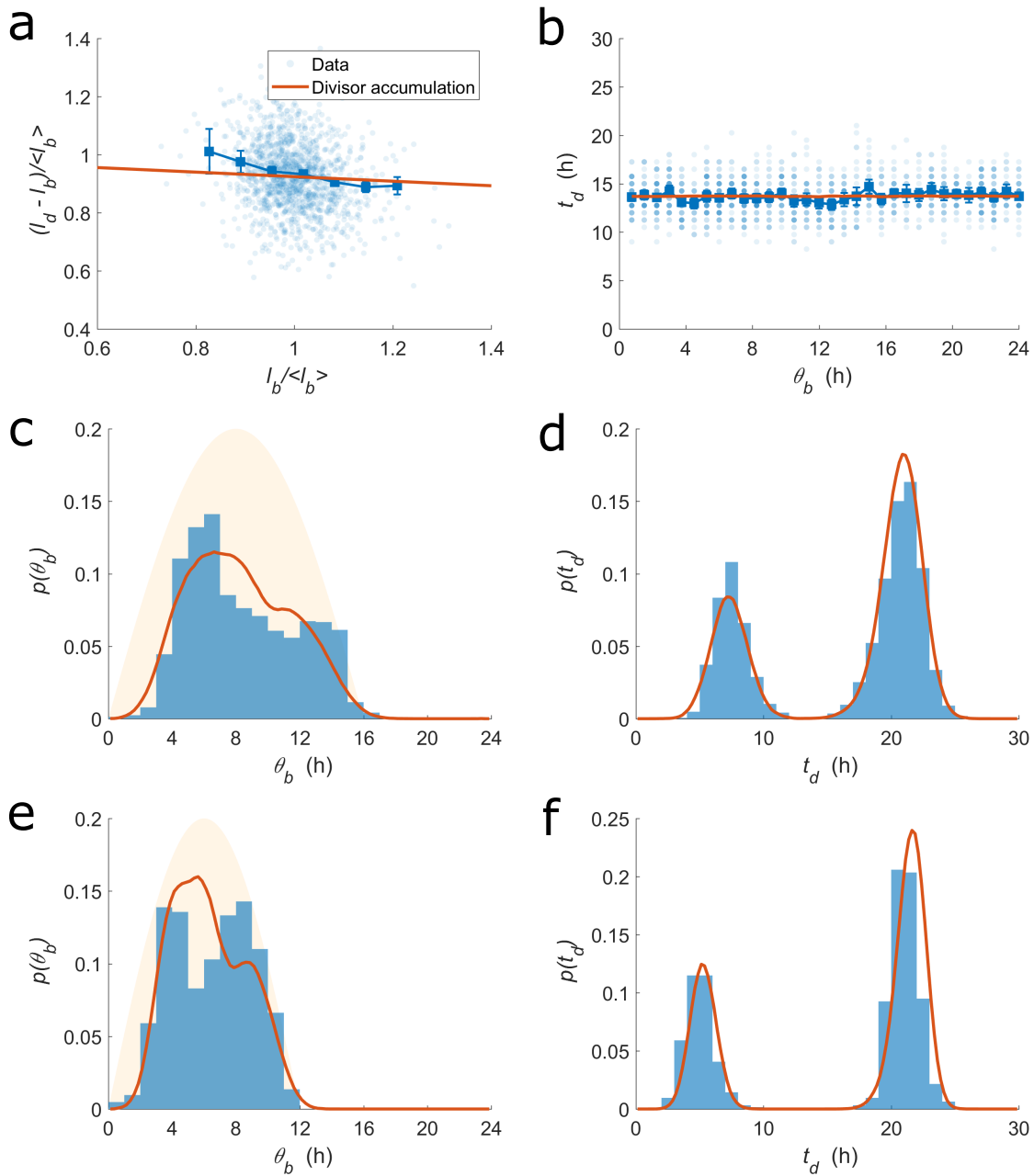
Figure 2: Divisor accumulation can describe division timing in the clock-deletion strain under LL (a,b), and under 16:8 (c,d) or 12:12 (e,f) LD. The correlations (a,b) and distributions (c-f) of the stochastic variables as defined in the caption of Fig. 1. $\langle \cdot \rangle$ denotes the average over all single-cells. Blue denotes data from Ref. (5). Red lines denote predictions of the divisor accumulation model. (a,b) Small points represent single-cell data. Large squares are averages binned according to the x-axis, with error bars showing the standard error of the mean. (c,e) Yellow shade shows the shape of the light intensity profile. Table S1 contains the parameter values used.
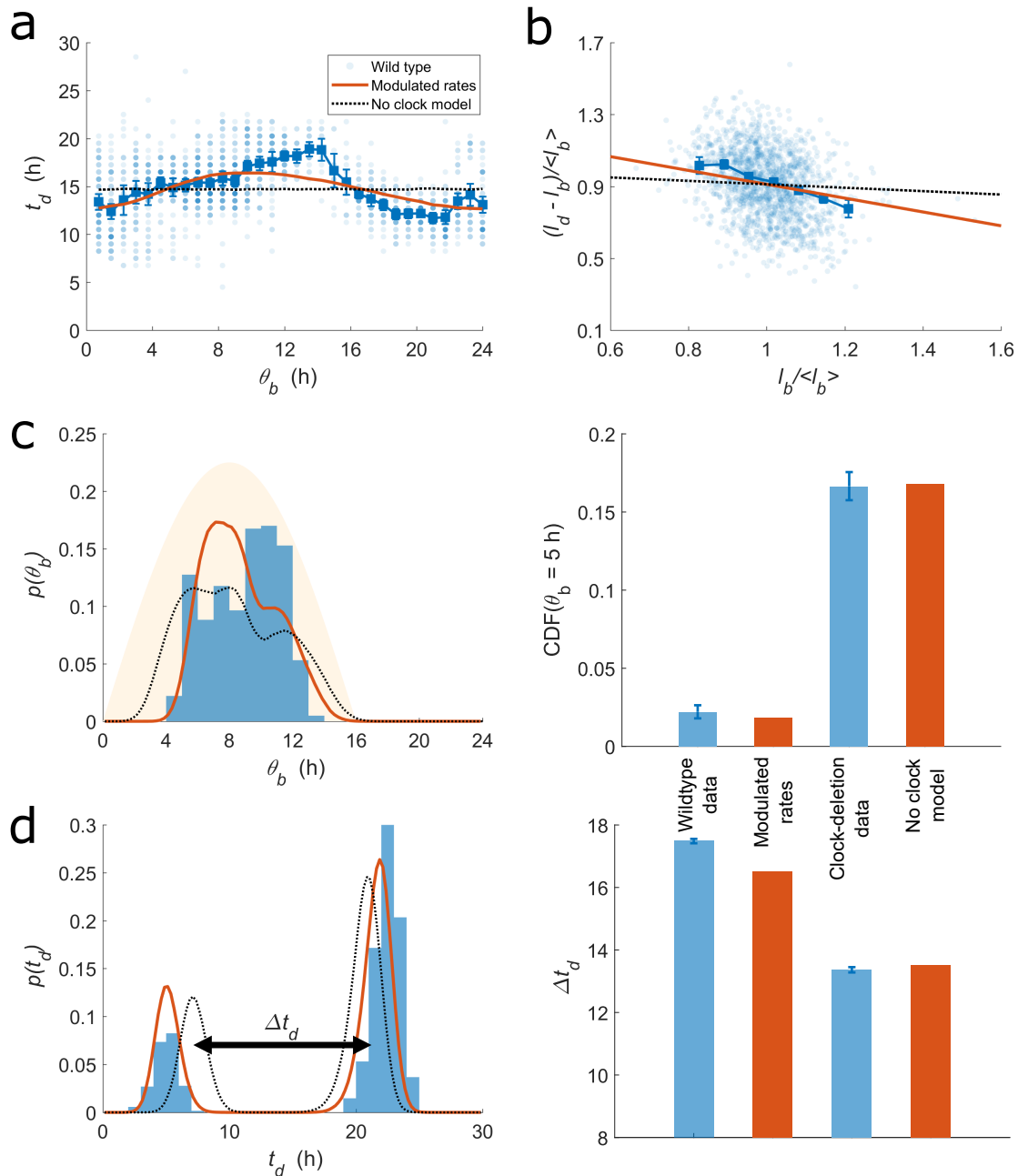
Figure 3: Divisor accumulation with modulated rates can describe division timing in the wild type strain under LL (a,b) and under 16:8 LD (c,d). Figure legends and axes labels are the same as in Fig. 2 except that red lines here denote predictions of the modulated rates model. Dashed black lines denote predictions of modulated rates model with $y(\theta) = 1$, equivalent to the divisor accumulation model, under the corresponding conditions. (c) The bar plot shows the cumulative fraction of divisions that have occured before the specified circadian phase five hours after dawn. (d) The bar plot shows the difference in the mean generation times of the short- and long-generation cells, Δt_d. Error bars in (c,d) show the standard deviation of the estimates due to sampling error calculated using bootstrapping. The results under 12:12 LD are shown in Fig. S5. The results for the gating model are shown in Fig. S6. Table S1 contains the parameter values used.
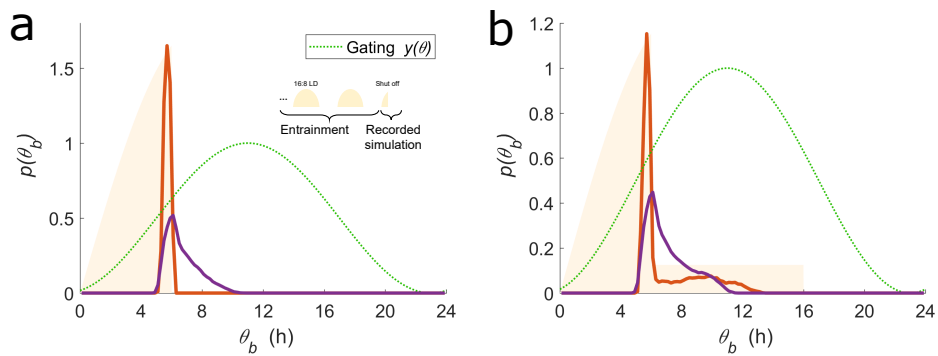
Figure 4: The modulated rates model robustly places divisions away from darkness, whereas the gating model does not. Predictions of the modulated rates (red) and gating (purple) models entrained under 16:8 LD and imaged for one cycle where the light is abruptly turned off (a) or down (b). The simulations used $y(\theta)$ best fit to the data of Ref. (5). The $y(\theta)$ in the gating model is shown in the green dotted line. Yellow shade shows the light profile during the imaging cycle. Inset shows the scenario that was numerically simulated.

LIST OF TABLES

	Circadian phase at peak activity (h)		
	Related experiment	Modulated rates	Gating
LL	-	12 ± 1	13 ± 1
16:8 LD	16 ± 1	14 ± 1	11 ± 1
12:12 LD	14 ± 1	12 ± 1	8 ± 1

Table 1: Distinguishing between the modulated rates and the gating models. The models predict different molecular players to implement the effects on division timing by the clock. The table shows the circadian phase at the peak of the bioluminescent reporter under the *kaiBC* promoter measured in the related experiment of Ref. (30), as well as the concentration of the divisor and effector in the modulated rates and gating models, respectively, as determined from the best fit values of φ in the two models (SM Section 1.